ON THE CALIBRATION OF THE DISTANCE MEASURING COMPONENT OF A TERRESTRIAL LASER SCANNER

P. Salo [a, *], O. Jokinen [a], A. Kukko[b]

[a] Department of Surveying, Helsinki University of Technology, P.O. Box 1200, 02015 TKK, Finland - Panu.Salo@TKK.fi

[b] Department of Remote Sensing and Photogrammetry, Finnish Geodetic Institute, P.O. Box15, 02431 Masala, Finland

Commission V, WG V/3

KEYWORDS: Component calibration, Terrestrial laser scanner, Robot tacheometer, Error function, Fourier analysis

ABSTRACT:

This paper deals with component calibration of a terrestrial laser scanner Faro LS880 HE80. The calibration is based on relative distance measurements and is focused on the distance measuring component of the scanner. The measurement range of 1-30 meters was divided into two parts according to the used sampling interval, and observations were compared to the results obtained with a robot tacheometer. The differences were analyzed by using Fourier transform techniques. The wavelengths, which yielded large amplitudes in the frequency space, were observed. The Fourier series yielded an error function for the relative distances measured with the laser scanner. The results indicated that the relative distance measurements were biased by both constant and periodic non-linear error, which we were able to correct using Fourier analysis. We also observed that the wavelengths of detected periodic errors often correlated with the wavelengths of the modulation frequencies of the instrument, or their harmonics.

1. INTRODUCTION

Laser scanning is a relatively new technology used in 3D mapping but is already widely used in different industry purposes. The technology offers products within a variety of different distance and accuracy ranges. New more developed scanners and softwares are released to the market one after an other. Users have most likely been interested in the accuracy of their scanner since the very first equipment and times of scanning. Total system calibration of a laser scanner is a quite challenging task, however. Lots of research has been done around the world to investigate the accuracy of different systems. Lichti and Licht (2006) and Lichti and Franke earlier (2005) have investigated the systematic error modeling of a terrestrial laser scanner. We have achieved the calibration of the distance measuring component of the terrestrial scanner in a relative measuring concept. An appropriate calibration setup was designed and implemented in the calibration baseline of the Institute of Geodesy of the Helsinki University of Technology on May 14, 2007. Tested terrestrial laser scanner was Faro LS880 HE80 and the reference equipment was tacheometer Leica TCA2003.

2. INSTRUMENTS

2.1 Terrestrial laser scanner

The tested terrestrial laser scanner was Faro LS 880 HE80 (S.No LLS 000500072) seen in Figure 1(a). The Faro LS scanner operates by emitting an infrared beam into the center of a rotating mirror. This deflects the laser beam on a vertical rotation around the environment being scanned. The beam is then reflected from the object surface back into the scanner, and the phase shift of the incoming light wave in relation to the emitted one is measured, thus giving the distance of the scanner from the object. Instead of a single pulse being reflected and the time of flight being measured, amplitude-modulated constant waves of multiple wavelengths are projected. The FARO LS splits the laser beam into three component parts operating on three different modulation wavelengths shown in Table 1 (Faro 2005).

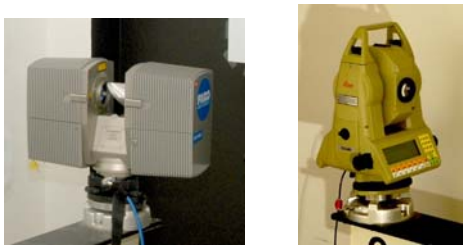

Figure 1. (a) Tested scanner Faro LS 880HE80, (b) reference equipment tacheometer Leica TCA2003.

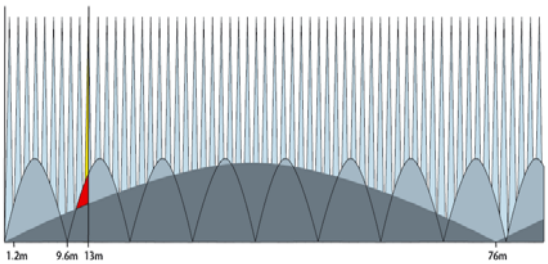

Figure 2. Modulation wavelengths of the Faro LS (Faro 2005).

Laser beam modulation lengths	1.2, 9.6 and 76.8 m
Points per second	120 000
Maximum distance	70 m
Linearity error at 10 m	3 mm
Vertical Field of View	320º
Horizontal Field of View	360º
Laser wavelength	785 nm
Laser power	22 mW

Table 1. Technical data of Faro LS 880HE80 (Faro, 2005; Lichti and Licht, 2006)

2.2 Reference equipment

The reference equipment used was Leica TCA2003 robot tacheometer (S.No. 438743) (Figure 1 b), which can track the motion of the prism. The distance measuring uncertainty is 1 mm + 1 ppm and the angle measuring accuracy is 0.15 mgon (Leica, 2003). Regarding that information, the ranging accuracy of the tacheometer was expected to be a degree better than that FARO LS could produce, and could thus provide appropriate reference for calibration

An ordinary Leica round prism (GPR1) was used as target in the tacheometer measurements. TCA2003 uses phase measurement of a modulated infrared laser beam in its range determination algorithm. Tacheometer provides automatic target recognition (ATR).

2.3 Other arrangements

The tested laserscanner Faro LS 880 HE80 was placed on a platform at the end of the about 80 meters long barline (Figure 4) and a reference equipment, a calibrated tacheometer Leica TCA2003, was placed on the platform at the other end. These instrument platforms were permanently mounted at both ends of the barline.

Measurement targets for both instruments were placed on a specially manufactured “target sled” seen in Figure 4. The sled has levelling screws, and tribrach adapters were tightly attached to the sled. Both measurement targets were attached to tribrachs on the sled. The centers of the two tribrach adapters on the sled were 14.9 cm apart.

The scanner target used for the calibration (see Figure 3 b) was made of a 5 mm thick aluminum plate with a target pattern printed on a piece of plain sticker paper. The target pattern had triangular shapes pointing towards the target center to provide reliable determination of the target center even at large distances. The target center was approximated from the laser data using the intensity image produced by the scanner.

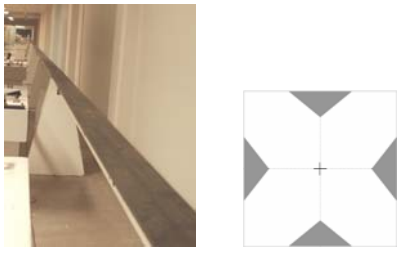

Figure 3. (a) The calibration barline used in the measurements, (b) Scanner target mounted on the prismholder.

3. MEASUREMENTS

The target sled was moved along the barline in a straight line at certain distance intervals, and distance measurements were made to measurement targets with both instruments from opposite directions. A steel measuring rod was used to guide the sled along a straight line. The straight line on top of the bar was measured and marked before the calibration by using the Leica TCA2003 tacheometer.

In the calibration phase, the first range measurements were made at a distance of about 1 m from the laser scanner. The target sled was then moved with approximately 10 cm distance intervals from the 1 m distance up to 5 m to reveal the phenomena in the shortest 1.2 m modulation wavelength, and also, due to the limited length of the steel rod guide, with approximately 45 cm intervals for distances from 5 m up to about 30 m from the scanner. The distances observed for the first target location with both instruments were used as reference distances $d_{0,L}$ and $d_{0,T}$ for the other measurements.

Figure 4. Measurement at a first distance about 1 m from the laser scanner. The tubular level that was used for levelling the sled is also shown in the image. Circles seen on the wall were not used in this calibration.

The carrier sled and prisms were accurately levelled at the sled location for the first distance using tubular levels. Subsequently, at each distance step along the bar line, the sled was levelled using a separate tubular level. Four single distance measurements were taken for each distance with both the laser scanner and tacheometer.

From the laser scanner data the target center was first determined using the intensity image of the data provided by the scanner, and then four closest distance recordings around the target center were used as calibration observations. That would result in a small uncertainty in relation to the exact target center location as a function of the angular resolution used for the scanning, but no significant effect to the distance (e.g ~1.5μm range error at 30 m distance for 0.018° (0.3 mrad) angular resolution).

The tacheometer provided directly horisontal distances between its origin and the targeted prism. Measurements were made either by using ATR or maximum signal of the prism was found manually. A precision distance measuring mode was used and four single measurements corrected for athmospheric effects were made at each measured distance.

The mean of the four tacheometer and TLS measurements for each target distance and distance differences for the observations were calculated. For both instruments, the result (mean value) of the measurements at the first distance was subtracted from the results of the measurements for the rest of

the target distances. The reference distance (i.e. a sort of origin) for the obtained relative distances was thus the first measurements about 1 m from the scanner.

Next, the relative distance differences of the tacheometer measurements were subtracted from the relative distance differences resulted from the laser scanner measurements. The comparison method was thus a relative one, not an absolute one. The standard deviation of the mean of four errors w (Figs. 6 and 7, and Eq. 4) was also calculated. For the error calculations, we considered the tacheometer measurements as exact.

4. FORMULAS AND ERROR FUNCTION BY FOURIER ANALYSIS

Calculations of the error function were carried out by using Fourier analysis (Joeckel and Stober, 1989, Thibos, 2003, Herman, 2002). Formulas are valid for equal sampling intervals.

Let $v_n=d_{n,L} - d_{n,T}$ where $d_{n,L}$ and $d_{n,T}$, n=0,…,N-1, are the relative distances measured by the laser scanner and tacheometer, respectively. The measurements were made at approximately equally spaced intervals $d_n=n\delta$, n=0,…,N-1, where δ=0.1 m for relative distances less than 4 m and δ=0.45 m for relative distances over 4 m. The discrete Fourier transform of the centered observations $u_n= v_n - \bar{v}$, n=0,…,N-1 is given by

$$U_k = \sum_{n=0}^{N-1} u_n exp(-i\omega_k n) = \sum_{n=0}^{N-1} u_n exp(-i\frac{2\pi k}{N\delta} d_n) \quad (1)$$

for k=0,…,N/2-1 (N is even). For the interval 0 m < d_n < 4 m and 4 m < d_n < 29 m , the highest maxima of the absolute value of U_k are located at wavelengths as explained in the following tables (Tables 2 and 3).

Relative distance 0-4 m	
ω_k/δ	Corresponding wavelength
20.4/m	0.31 m
3.14/m	2.0 m
1.57/m	4.0 m

Table 2. Angular frequencies and wavelengths of highest maxima at relative distances (0-4 m).

Relative distance 4-29 m	
ω_k/δ	Corresponding wavelength
0.24/m	25.6 m
5.14/m	1.22 m

Table 3. Angular frequencies and wavelengths of highest maxima at relative distances (4-29 m).

The Fourier series yields a correction function for the relative distances measured by the laser scanner. The correction function is given by:

$$\hat{v}_n = \bar{v} + \frac{2}{N}\sum_{k=1}^{M} |U_k| \cos(\omega_k n + \varphi_k) = \bar{v} + \frac{2}{N}\sum_{k=1}^{M} a_k \cos(\omega_k n) + b_k \sin(\omega_k n) \quad (2)$$

where φ_k is the phase angle of U_k, M is the number of highest maxima included (3 maxima at relative distances 0-4 m and 2 maxima at relative distances 4-29 m),

$$a_k = \sum_{n=0}^{N-1} u_n \cos(\omega_k n),$$
$$b_k = \sum_{n=0}^{N-1} u_n \sin(\omega_k n). \quad (3)$$

5. RESULTS

All measured relative distance errors are shown in Figure 5. The y-axis describes the relative distance error of the scanner $v_n=d_{n,L} - d_{n,T}$, and the x-axis describes the relative distances where the reference distance is about 1 m away from the scanner. Relative distances of the x-axis are distances from the reference distance.

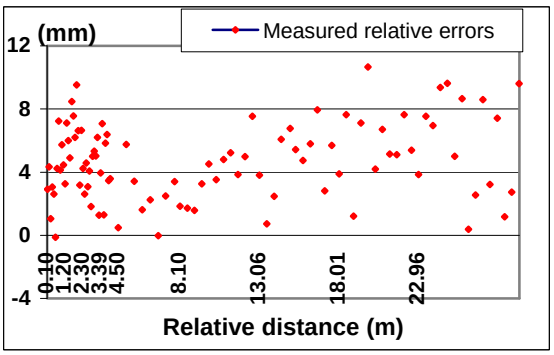

Figure 5. Measured relative distance errors.

Figure 6 illustrates measured relative errors between relative distances 0 and 4 m, meanwhile Figure 7 shows comparable relative errors for relative distances between 4 m and 29 m. The standard deviation w_n (see Eq. 4) of the mean of relative errors shown in graphics as error bars (Figs. 6 and 7) is calculated from the four scanner measurements and from the mean value of relative tacheometer measurements at each relative distance. Scanner vectors at each relative distance were calculated so that the 1st measurement at the 1 m reference distance $d_{0_1,L}$ was subtracted from the 1st measurement of nth distance $d_{n_1,L}$, 2nd measurement of the reference distance $d_{0_2,L}$ was subtracted from the 2nd measurement of nth distance $d_{n_2,L}$ and so on. Corresponding relative distances $d_{n,T}$ for the tacheometer were subtracted from these results. Average a_n of four differences were counted and then corresponding w_n.

$$w_n = \frac{\sqrt{\left(\left(\left(d_{n_1,L} - d_{0_1,L}\right) - d_{nT}\right) - a_n\right)^2 + \ldots + \left(\left(\left(d_{n_4,L} - d_{0_4,L}\right) - d_{nT}\right) - a_n\right)^2 / 3}}{2} \quad (4)$$

where $a_n = \frac{\left(\left(d_{n_1,L} - d_{0_1,L}\right) - d_{nT}\right) + \ldots + \left(\left(d_{n_4,L} - d_{0_4,L}\right) - d_{nT}\right)}{4}$

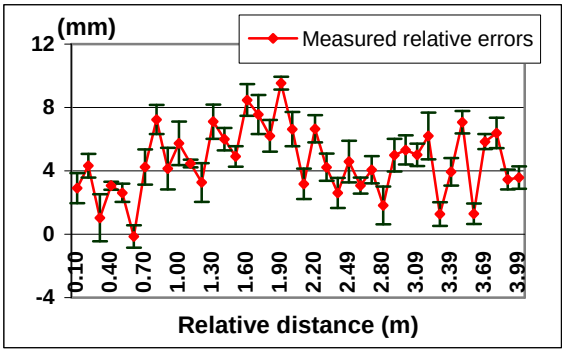

Figure 6. Measured relative errors at relative distances (0-4 m) and their error bars.

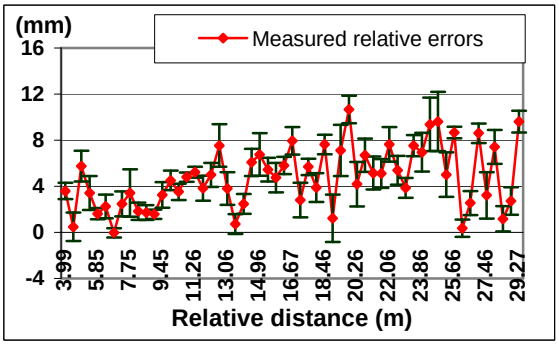

Figure 7. Measured relative errors at relative distances (4-29 m) and their error bars.

In Figure 6 the relative distances are shown within the range of 0-4 m with sampling interval of 0.1 m. In Figure 7 the relative distances of 4-29 m are shown, and the sampling interval was approximately 0.45 m.

Figures 8 and 9 describe the obtained error functions in blue (see Eq. 2) solved by Fourier analysis. The other curve in red in the graphs is the same relative error at relative distances measured by laser scanner and tacheometer as in Figs. 6 and 7 but without error bars.

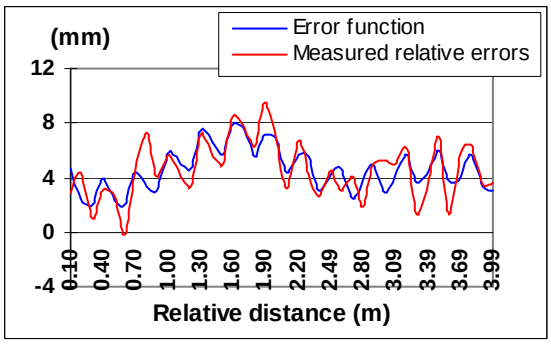

Figure 8. Graph of the error function and measured relative errors at relative distances (0-4 m).

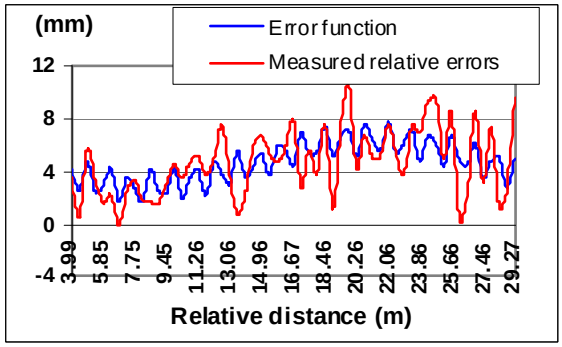

Figure 9. Graph of the error function and measured relative errors at relative distances (4-29 m).

Adjustment residuals e_n seen in Figs. 10 and 11 are calculated from the data illustrated in Figs. 8 and 9. The residuals are the adjusted errors subtracted by the measured errors at relative distances (0-4 m) and (4-29 m). Figure 10 shows the residuals of the 0.1 m sampling intervals and Figure 11 illustrates the residuals of the 0.45 m sampling intervals. The standard errors of the unit weight m_0 in both interval adjustments are described in Eq. 5 and in Table 4.

e_n= residual= adjusted relative error-measured relative error

$$m_0 = \sqrt{\frac{\sum e_n^{\,2}}{N-u}}, \qquad (5)$$

where u=2M+1

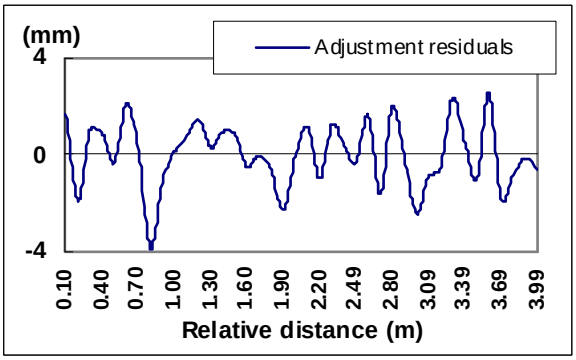

Figure 10. Adjustment residuals at relative distances (0-4 m).

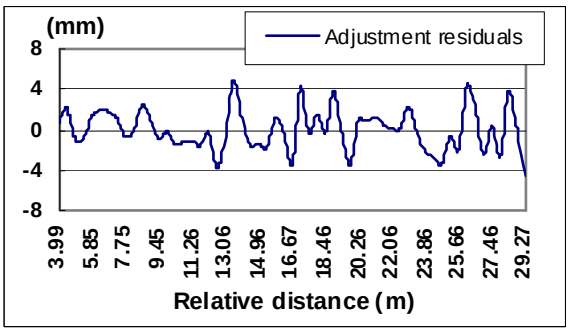

Figure 11. Adjustment residuals at relative distances (4-29 m).

Relative distance	Standard error of the unit weight (m_0) in adjustment
0-4 m	1.5 mm
4-29 m	2.2 mm

Table 4. Standard errors of the unit weight m_0 in adjustments.

Figure 12 describes the sampling intervals used for the calibration measurements as a function of distance. A couple of gross errors in the sled movements were taken place during the measurements.

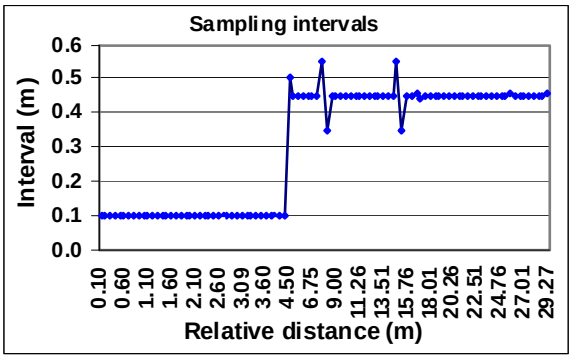

Figure 12. Sampling intervals at relative distances (0-29 m).

6. CONCLUSIONS

Periodic errors found in this study can be corrected with the error function calculated by Fourier analysis.

Single measured errors of relative distances were always positive or close to zero and at maximum of about 10 mm (Figs. 6 and 7). We noticed that errors included a constant error and a nonlinear error. Constant error $\overline{v}$ (see Eq. 2) with 10 cm sampling intervals (0-4 m) was 4.6 mm and with approximately 45 cm intervals (4-29 m) 4.7 mm. According to the error function (Figs. 8 and 9) the largest error was about 8 mm.

The wavelengths of periodic errors often correlated with the wavelengths of the modulation frequencies of the instrument, or their harmonics. The evaluated wavelengths of periodic errors for relative measurements with 10 cm sampling intervals (0-4 m) were 0.31 m, 2 m and 4 m (Table 2). For measurements with approximately 45 cm intervals (4-29 m), the wavelengths evaluated were 1.2 m and 25.6 m (Table 3). One reason for not getting equal wavelengths for both relative distance areas may occur because sampling intervals were different and calculations were made with relatively small data. Therefore errors, or inaccuracies in calculated wavelengths are possible. According to Lichti and Licht (2006) wavelengths of cyclic error terms of Faro HE scanner are 0.6 m, 4.8 m and possibly 38.4 m, which correspond to one half of the modulated wavelengths.

Future research is needed to find out the original causes of the observed periodic errors. Possible reasons include non-linearity of the electrical circuit of the phase measurement system, crosstalk phenomena inside the instrument or extra reflections between the target and the instrument.

ACKNOWLEDGEMENTS

The research described in this paper is part of the Finnish KITARA programme consortia project “Use of ICT 3D measuring techniques for high quality construction”. The aim of the programme is to strengthen basic research expertise in the fields of mechanical, civil, and automation engineering through the application of ICT.

Authors are grateful to D.Sc. (Tech.) Jaakko Santala for planning the calibration method, Veli-Matti Salminen for proper technical arrangements, Lic.Sc. (Tech.) Petteri Pöntinen, Laboratory Technician Antero Tihveräinen and M.Sc. (Tech.) Dan Häggman who helped with the measurements and Prof. Martin Vermeer for quidance and advises regarding the applied methodology.

REFERENCES

Faro, 2005. FARO laser scanner LS: Recording reality's digital fingerprint. http://www.faro.com/FaroIP/Files/File/Brochures/UK_brochure_FARO_ScannerLS.pdf (accessed 17.4.2008)

Herman, R..L., 2002. Fourier Analysis of Time Series, UNC Wilmington. http://people.uncw.edu/hermanr/signals/Notes/Signals.htm (accessed 17.4.2008)

Joeckel, R. Stober, M, 1989. Elektronische Entfernungs- und Richtunsmessung. Stuttgart, pp. 123-127.

Leica, 2003. Leica TPS -System 1000 manual. Version 2.3.

Lichti D. and Franke J. 2005. Self-Calibration of the IQSUN 880 Laser Scanner. In: Optical 3D Measurement Techniques VII, Vienna, Austria, Vol. I, pp. 112-121.

Lichti D. and Licht M. 2006. Experiences with terrestrial laser scanner modeling and accuracy assessment. IAPRS Volume XXXVI, PART 5, Dresden 25-27 September 2006.

Thibos, L.N., 2003. Fourier analysis for beginners. School of Optometry, Indiana University, Bloomington, IN 47405. http://research.opt.Indiana.edu/Library/FourierBook/ch04.html (accessed 17.4.2008)